DOI: 10.1002/ejic.201000513

Solution Route to PbSe Films with Enhanced Thermoelectric Transport Properties

Zhengliang Sun,[a,b] Shengcong Liufu,*[a] Xihong Chen,[a] and Lidong Chen[a]

Keywords: Thermoelectrics / Thin films / Solution synthesis / Lead / Selenium

Thermoelectric (TE) PbSe thin films, assembled by nanoparticles (100–400 nm), were synthesized by a facile solution route. Results of scanning and transmission electron microscopy investigations revealed the high compactness of the PbSe films with highly crystallized nanoparticles. Electrical transport properties including low resistivity (0.01 Ωcm), high Seebeck coefficient (324 μVK^{-1}), and high carrier mobility (195 $cm^2V^{-1}S^{-1}$) of the PbSe films at 300 K are superior to those of films synthesized by other solution routes and comparable with those of films prepared by vacuum-based methods. The PbSe films exhibit a maximum thermoelectric power factor (31.5 $\mu Wcm^{-1} K^{-1}$) at 440 K, which is larger than that of the bulk PbSe by 57 %, making the assembled PbSe films promising TE films.

Introduction

Pursuing a high figure of merit, ZT (defined as $S^2\sigma T/\kappa$, where S is the Seebeck coefficient, σ is the electrical conductivity, T is the absolute temperature, and κ is the thermal conductivity), has become the most important concern for thermoelectrics researchers in recent decades to develop high-energy-conversion devices for solid-state cooling and power generation.[1–4] Theoretical modeling and experimental proof-of-principle indicate that nanostructuring is a promising means to realize a tremendous enhancement in the ZT value.[5–10] The enhanced boundary scattering introduced by nanograins can effectively depress the thermal conductivity; a ZT value as high as 2.4 has been achieved in Bi_2Te_3/Sb_2Te_3 superlattice thin films caused by the strong reduction of the κ value.[5] In addition, the quantum effects that appear at characteristic sizes can improve the power factor (PF, defined as $S^2\sigma$). It was reported that the PF of Bi_2S_3 thin films with c-axis-oriented nanorod assemblies is 12 times larger than the corresponding value for bulk Bi_2S_3 at room temperature.[11] Besides the improvement in efficiency, developing low-cost and simple manufacturing processes have attract technological interest.[12,13] Previous work on nanostructured TE materials with high efficiency often depended on high-cost vacuum-based techniques.[2,5,14] Thus, it is still a challenge to develop a scalable strategy for preparing nanostructured TE materials with high efficiency.

[a] CAS Key Laboratory of Materials for Energy Conversion, Shanghai Institute of Ceramics, Chinese Academy of Science, 1295 Dingxi Road, Shanghai 200050, P. R. China
Fax: +86-21-52413122
E-mail: scliufu@hotmail.com
[b] Graduate School of the Chinese Academy of Science, 19 Yuquan Road, Beijing 100049, P. R. China
Supporting information for this article is available on the WWW under http://dx.doi.org/10.1002/ejic.201000513.

Lead selenides (PbSe) have been chosen as our research target to explore an alternative strategy for both their excellent TE properties at middle-range temperatures and abundant previous work on the solution route for preparing them.[15–18] Previous work on PbSe films prepared by the solution route focused on two main procedures. One route, drop-casting monodisperse PbSe nanocrystals into superlattice films,[19] enhanced the Seebeck coefficient significantly due to the sharp increase in the density of states (DOS); however, the electrical conductivity dropped by one order of magnitude relative to the bulk PbSe due to the dramatic decrease in the hole mobility (ca. 0.1 cm^2/Vs), which might be caused by the unexpected interparticle spacing. When the second route, that is, depositing PbSe nanocrystalline films using chemical bath deposition (CBD),[20] was employed, low crystallization and unexpected impurity introduced by homogeneous nucleation and growth deteriorated the TE transport properties. In addition, extra treatments (such as annealing) often complicated the synthetic process. In this work, we prepared PbSe films assembled with highly crystallized nanoparticles (100–400 nm) by a solution method through elaborate design of the precursor solution. The PbSe films exhibited TE properties better than those of polycrystalline bulk PbSe and comparable with those of the vacuum-based PbSe films.

Results and Discussion

Excellent TE performance in thin films can be achieved by assembly of compact building blocks with high quality.[11] As for the solution route, the design of the precursor solution plays a vital role in the ion-by-ion assembly of the targeted films, which could ensure a high quality. In the traditional CBD process for PbSe films, Se^{2-} was commonly

accessed by hydrolysis of Na_2SeSO_3 at high pH value (> 13), which was often accompanied by unexpected impurities (e.g. oxides) and low crystallization. In the present work, Se^{2-} was easily accessed by a redox reaction of Na_2SeSO_3 at a much lower pH value (ca. 8), in which ascorbic acid (AA) was introduced as reductant. As for the Pb precursor, $Pb(NO_3)_2$ was chosen, and nitrilotriacetic acid (NTA) was used to control the release of Pb^{2+}. Si wafers were used as substrate after being oxidized by piranha solution. According to the theory of crystal growth,[21,22] no nucleation occurs in a solution with low supersaturation, homogeneous nucleation occurs at high supersaturation, and film formation from heterogeneous nucleation is possible in the intermediate supersaturation region. In our work, the supersaturation degree can be easily controlled by the concentration of NTA to obtain high-quality PbSe films. As indicated in Figure 1, loose and noncontinuous PbSe films are formed on the deposited side (marked A in Figure 1a) of the substrate, and no films are formed on the other side (marked B in Figure 1a) when the Pb^{2+}/NTA ratio is below 1:10 (Figure 1b). The films here were formed as a result of homogeneous nucleation in the solution. On the other hand, PbSe films formed on side A of the substrate with Pb^{2+}/NTA = 1:15 (Figure S1) are composed of continuous films and surface particles. PbSe films formed on side B of the substrate with Pb^{2+}/NTA = 1:15 (Figure 1c, d) are composed of continuous films without particle structures on the surface. This is due to heterogeneous nucleation at the surface of the substrate. The following discussion is based on this continuous film.

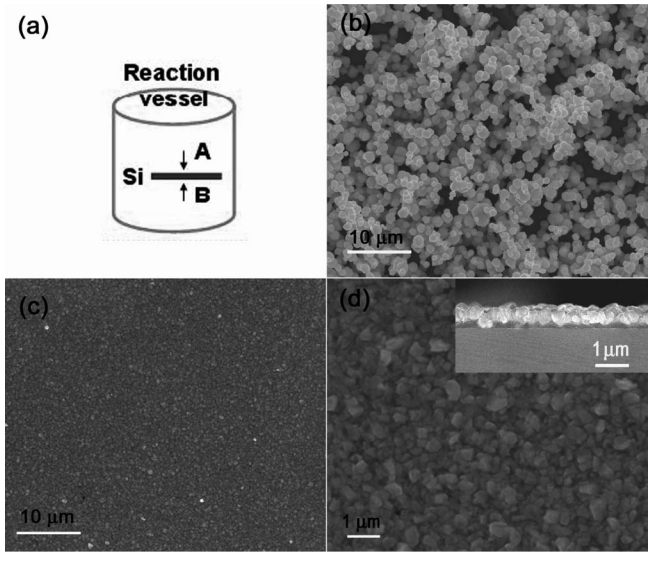

Figure 1. Sketch of the reaction (a); SEM images of the synthesized PbSe films with Pb^{2+}/NTA = 1:10 on side A (b), Pb^{2+}/NTA = 1:15 on side B (c and d) with different magnifications. The inset in (d) shows the corresponding cross-sectional image.

The high quality of a typical PbSe film was confirmed by the XRD (Rigaku RINT 2000, Cu-K_α) pattern displayed in Figure 2a, in which all the peaks match well those of the cubic phase of lead selenide with the $Fm\bar{3}m$ space group (JCPDS, 06–0354). This result indicates that highly crystallized PbSe films can be directly assembled on a Si substrate by rational design of the precursor solution, which shows the simplicity of the solution route for preparing PbSe films (no extra annealing process is needed). The purity of the synthesized PbSe films was reconfirmed by electron probe microanalysis (EPMA), as shown in Figure 2b, which also indicates that the atomic ratio of lead and selenium is close to 1:1. From the surface scanning electron microscopy images (SEM, JSM-6390) in Figure 1c and Figure 1d, it can be seen that the film is homogeneous and consists of nanoparticles ranging from 100 to 400 nm. From the cross-sectional SEM image inserted in Figure 1d, the thickness of the film is uniform with a value of about 700 nm. The compactness and uniformity facilitate uniform carrier-charge transport across the nanostructured film. Figures 3a and b display the TEM images of the PbSe films. The observed lattice spacings of 0.355 nm and 0.217 nm correspond to the 1–11 and 220 planes of PbSe, confirming the high crystallinity of the assembled nanoparticles.

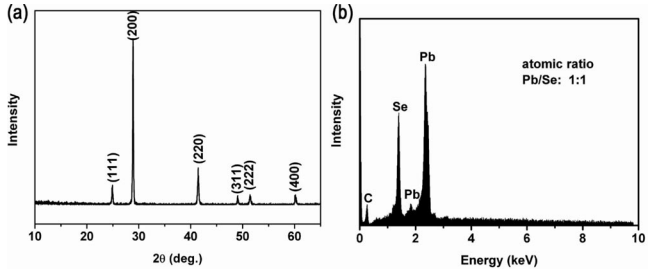

Figure 2. XRD pattern and EPMA plot of the synthesized film, indicating the high crystallinity and purity of the synthesized film with atomic ratio of Pb/Se close to 1:1.

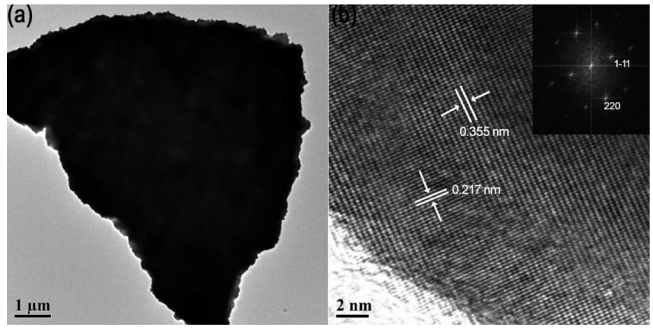

Figure 3. TEM images with low magnification (a) and high magnification (b), the inset shows the corresponding fast Fourier transform (FFT) image.

Figure 4 shows the temperature (T) dependence of TE transport properties of PbSe films, including the electrical resistivity ($\rho = 1/\sigma$), S, and PF. The influence of the Si substrate on the TE properties can be eliminated by the insertion of an insulating oxide layer between the silicon wafer and PbSe films. The electrical resistivity of the assembled PbSe films at 300 K is 0.01 Ωcm, which is much lower than those of other solution-route PbSe films (1–10^6 Ωcm).[19,20] The enhanced electrical property arises from the increase in the carrier mobility, reaching 195 $cm^2 V^{-1}S^{-1}$, which is much larger than the corresponding value for nanocrystal PbSe

films (ca. 0.1 cm^2/Vs).[19] Positive values of S indicate p-type conduction, which is expected for PbSe. The S value at room temperature (324 μVK^{-1}, with a carrier concentration of 3.3×10^{18} cm^{-3}) is larger by 62% relative to that found for polycrystalline bulk PbSe with a comparable carrier concentration of 3.2×10^{18} cm^{-3}.[23] Quantum effects embedded in the nanostructured films, such as energy filters, might be responsible for the improved Seebeck coefficient.[11,24] Because of the improved electrical transport, the PF (S^2/ρ) for the PbSe films reaches 10 $\mu Wcm^{-1} K^{-1}$, which is larger than the corresponding value for bulk PbSe (5–7 $\mu Wcm^{-1} K^{-1}$)[25] and comparable to that of vacuum-based PbSe films.[26]

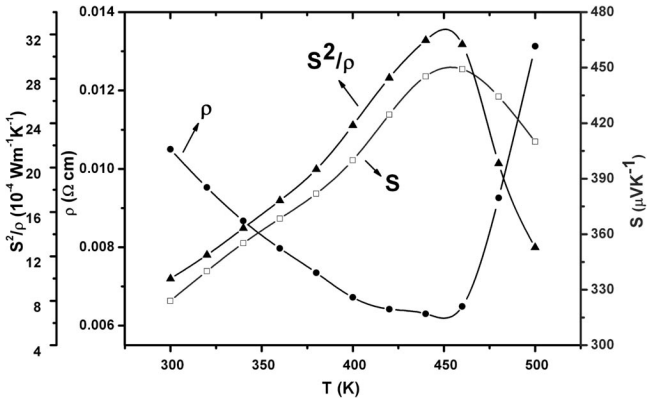

Figure 4. Temperature dependences of the electrical resistivity (ρ, circles), Seebeck coefficient (S, squares), and the thermoelectric power factor (S^2/ρ, triangles) of the PbSe films.

From Figure 4, a linear decrease in ρ with temperature in the range 300–450 K suggests the presence of an activation barrier at the grain boundary between the nanoparticles.[27] After 450 K, ρ increases sharply; this could be attributed to two possible mechanisms. One mechanism is the desorption of oxygen as proposed by Damodara Das et al.[28] For air-exposed PbSe films, oxygen atoms and/or molecules are adsorbed on the surface of the films, and they act as p-type dopants. Desorption of oxygen from the film surface at high temperature usually decreases the carrier concentration in a "p" type sample and thus increases the resistance of the sample. The other is a sharp decrease in mobility due to creation of defects at elevated temperature as proposed by Smith.[29] It was argued that, in lead chalcogenides, defects will be created at high temperature. These defects can act as scattering centers for the carriers, bringing down the mobility of the carriers, which also results in a sharp increase of the resistivity. Thus, as a result of these mechanisms, the resistivity increases sharply at high temperature. Moreover, due to the decreased mobility, we also observe a slight drop of the Seebeck coefficient from 450 μVK^{-1} at 460 K to 410 μVK^{-1} at 500 K. Combining the increase in resistivity and the variation of the Seebeck coefficient with temperature, the PF factor can reach 31.5 $\mu Wcm^{-1} K^{-1}$ at 440 K, which is larger than the corresponding value for bulk polycrystalline PbSe at the same temperature by 57%.[30] In addition, effective phonon scattering at the interface between the boundaries of the nanograins will also contribute to the enhancement of the ZT value. Therefore, PbSe films assembled by this solution route are a promising bolster for microheating and cooling devices.

Conclusions

High-quality PbSe films were synthesized by a facile solution route by rational design of the precursor solution. The PbSe films exhibit good electrical conduction properties and meanwhile maintain a large Seebeck coefficient. The enhancement of thermoelectric transport properties mainly results from high carrier mobility across embedded compacted highly crystallized nanoparticles. The TE power factor of the PbSe films is larger than that of bulk PbSe. The improved TE properties suggest that the assembled PbSe film is a promising TE film.

Experimental Section

Synthesis of PbSe Thin Films: A typical precursor solution was composed of $Pb(NO_3)_2$ (2 mL, 0.1 M), nitrilotriacetic acid (NTA) (30 mL, 0.1 M), ascorbic acid (AA) (2 mL, 0.5 M), and freshly made Na_2SeSO_3 (2 mL, 0.1 M). The pH value of the solution was adjusted to about 8 by the addition of a few drops of diluted ammonia. All of the reagents were of analytical grade (Alfa Aesar) and were used without further purification. Before reaction, the Si substrates were immersed in piranha solution [a 30:70 (v/v) mixture of 30% H_2O_2 and concentrated H_2SO_4] at 80 °C for 30 min. After that, the Si substrates were washed with deionized water and then immersed in the middle of the solution to favor the nucleation and growth of PbSe films. The solution was kept covered with polyethylene film to prevent the evaporation of water and placed in a water bath maintained at 70 °C for 3 h. At the end of the experiment, the films were removed from the bath, rinsed carefully with deionized water, and then dried naturally.

Film Characterization: The crystalline structures of PbSe thin films were analyzed with an X-ray diffractometer (XRD; Rigaku RINT 2000) operating with Cu-K_α radiation at 40 kV/40 mA. Morphologies of the samples were analyzed by scanning electron microscopy (JSM-6390). The electron probe microanalysis (EPMA) results were recorded with a 8705QH2 instrument. The synthesized film was scraped from the Si substrate and dispersed onto a carbon-coated Cu grid, and then transported into a JEOL200CX instrument for TEM analysis. The dark electrical resistivity and the carrier concentration of the PbSe films were measured by a four-point probe method in van der Pauw configuration with an Accent HL5500 Hall System. Silver paste was applied to provide ohmic contact with PbSe films. For the measurement of the Seebeck coefficient, two Pt–Pt/Rh thermocouples were attached to both ends of the PbSe thin films, and temperature gradients of 3–5 K were generated by a film heater at one end. The Seebeck coefficient was then obtained from the slope of a plot of thermoelectromotive force versus temperature difference.

Supporting Information (see footnote on the first page of this article): SEM image of the synthesized PbSe films with Pb^{2+}/NTA ratio 1:15 on side B.

Acknowledgments

Financial support from the National Science Foundation of China (Grant Nos. 50702069, 50821004, and 10QA1407700) is gratefully acknowledged.

[1] L. D. Hicks, M. S. Dresselhaus, *Phys. Rev. B* **1993**, *47*, 12727–12732.
[2] T. C. Harman, P. J. Taylor, M. P. Walsh, B. E. LaForge, *Science* **2002**, *197*, 2229–2232.
[3] K. F. Hsu, S. Loo, F. Guo, W. Chen, J. S. Dyck, C. Uher, T. Hogan, E. K. Polychroniadis, M. G. Kanatzidis, *Science* **2004**, *303*, 818–821.
[4] B. Poudel, Q. Hao, Y. Ma, Y. Lan, A. Minnich, B. Yu, X. Yan, D. Wang, A. Muto, D. Vashaee, X. Chen, J. Liu, M. S. Dresselhaus, G. Chen, Z. F. Ren, *Science* **2008**, *320*, 634–638.
[5] R. Venkatasubramanian, E. Siivola, T. Colpitts, B. O'Qiunn, *Nature* **2001**, *413*, 597–602.
[6] E. Quarez, K. F. Hsu, R. Pcionek, N. Frangis, E. K. Polychroniadis, M. G. Kanatzidis, *J. Am. Chem. Soc.* **2005**, *127*, 91779190.
[7] W. Wang, B. Poudel, J. Yang, D. Z. Wang, Z. F. Ren, *J. Am. Chem. Soc.* **2005**, *127*, 13792–13793.
[8] M. S. Dresselhaus, G. Chen, M. Y. Tang, R. G. Yang, H. Lee, D. Z. Wang, Z. F. Ren, J. P. Fleurial, P. Gogna, *Adv. Mater.* **2007**, *19*, 1043–1053.
[9] X. B. Zhao, X. H. Ji, Y. H. Zhang, T. J. Zhu, J. P. Tu, X. B. Zhang, *Appl. Phys. Lett.* **2005**, *86*, 06211–06213.
[10] X. F. Tang, W. J. Xie, H. Li, W. Y. Zhao, Q. J. Zhang, M. Niino, *Appl. Phys. Lett.* **2007**, *90*, 012102–012104.
[11] S. C. Liufu, L. D. Chen, Q. Yao, C. F. Wang, *Appl. Phys. Lett.* **2007**, *90*, 112106–112108.
[12] X. F. Qiu, L. N. Austin, P. A. Muscarella, J. S. Dyck, C. Burda, *Angew. Chem. Int. Ed.* **2006**, *45*, 5656–5659.
[13] Y. M. Lin, O. Rabin, S. B. Cronin, J. Y. Ying, M. S. Dresselhaus, *Appl. Phys. Lett.* **2002**, *81*, 24032405.
[14] L. Da Silva, M. Kaviany, C. Uher, *J. Appl. Phys.* **2005**, *97*, 114903.
[15] T. Mokari, S. E. Habas, M. J. Zhang, P. D. Yang, *Angew. Chem. Int. Ed.* **2008**, *47*, 5605–5608.
[16] S. Gorer, A. Albu-Yaron, G. Hodes, *Chem. Mater.* **1995**, *7*, 1243–1256.
[17] H. Saloniemi, T. Kanniainen, M. Ritala, M. Leskela, R. J. Lappalaninen, *J. Mater. Chem.* **1998**, *8*, 651–654.
[18] Z. Hens, E. S. Kooij, G. Allan, B. Grandidier, D. Vanmaekelbergh, *Nanotechnology* **2005**, *16*, 339–343.
[19] R. Y. Wang, J. P. Feser, J. S. Lee, D. V. Talapin, R. Segalman, A. Majumdar, *Nano Lett.* **2008**, *8*, 2283–2288.
[20] F. L. Zhou, X. M. Li, X. D. Gao, J. J. Qiu, *Int. J. Inorg. Mater.* **2009**, *24*, 778–782.
[21] K. Sawada, *Pure Appl. Chem.* **1997**, *69*, 921–928.
[22] Y. F. Gao, Y. Masuda, K. Koumoto, *Chem. Mater.* **2003**, *15*, 2399–2410.
[23] H. Abrams, R. N. Tauber, *J. Appl. Phys.* **1969**, *40*, 3868.
[24] J. Martin, L. Wang, L. D. Chen, G. S. Nolas, *Phys. Rev. B* **2009**, *79*, 115311.
[25] V. Jovovic, S. J. Thiagarajan, J. West, J. P. Heremans, T. Story, Z. Golacki, W. Paszkowicz, V. Osinniy, *J. Appl. Phys.* **2007**, *102*, 043707.
[26] E. I. Rogacheva, T. V. Tavrina, O. N. Nashchekina, S. N. Grigorov, K. A. Nasedkin, M. S. Dresselhaus, S. B. Cronin, *Appl. Phys. Lett.* **2002**, *80*, 2690–2692.
[27] Z. Dashevsky, R. Kreizman, M. P. Dariel, *J. Appl. Phys.* **2005**, *98*, 094309.
[28] V. Damodara Das, K. Seetharama Bhat, *Phys. Rev. B* **1989**, *40*, 7696.
[29] R. A. Smith, *Physics* **1954**, *20*, 910–929.
[30] M. M. Ibrahim, S. A. Saleh, E. M. M. Ibrahim, A. M. Abdel Hakeem, *J. Alloys Compd.* **2008**, *452*, 200–204.

Received: May 10, 2010
Published Online: August 18, 2010

